Variation of Counterelectrode Size to Control Current Distribution in Parallel Plate Cells

Alonso Lozano-Morales,[1] Heather McCrabb,[1] E. Jennings Taylor[1] and Alan C. West[2]*
[1]Faraday Technology, Inc., 315 Huls Drive, Clayton, OH USA
[2]Department of Chemical Engineering, Columbia University, New York, NY USA

The effect of counterelectrode radius on uniformity in plating or electrochemical machining a disk-shaped electrode is shown. It is assumed that both the anode and cathode are located on parallel plates, which are otherwise insulating. The optimal ratio of electrode radii is reported as a function of separation distance. Results are compared to electrochemical machining studies of stainless steel 303 and Hastelloy X in a sodium nitrate electrolyte.

Keywords: *electrodeposition, current distribution, parallel plate electrodes*

Introduction

When plating or electrochemically etching a substrate that is partially covered with an insulating material, it is well known that edge effects can cause the current density distribution to be very nonuniform,[1] even when the electrode is recessed slightly due to the finite thickness of the insulating material.[2] Numerical methods to optimize, for example, the use of current thieves or shields exist, and very sophisticated theoretical treatments are available.[3] A common, practical scenario is one in which a counterelectrode is placed parallel to the working electrode at a relatively small distance, and the introduction of specially designed shields or thieves cannot be economically justified because, for example, only a few pieces need to be machined or plated. When more elaborate cell-design changes are not justified, the masking of the counterelectrode may be a simple approach to improve uniformity, but to our knowledge, the optimal masking has not been reported.

A schematic of the cell that is considered is shown in Fig. 1. For simplicity, it is assumed that the active region, where plating or electrochemical machining is desired, is confined to a disk of radius r_{we}. The parallel counterelectrode is separated by a distance h. It is assumed that counterelectrode can be masked, and the present study addresses the question of what is the best counterelectrode radius r_{ce}. The ratio r_{ce}/r_{we} is shown to depend strongly on h/r_{we}.

The optimization of the ratio was based on minimizing nonuniformities in current distribution and was achieved by simulation of the primary current distribution. Factors such as mass transfer and electrode kinetics, as well as geometric complications such as patterning may cause the realizable current density distribution to deviate from predictions. Often however, such complications increase uniformity in current distribution.

Numerical simulations are compared to electrochemical machining experiments, the application for which the simulations were originally performed. The simulations are shown to be in accord with experiments, even though electrochemical machining may occur under operating conditions that may not *a priori* be expected to match the assumptions of a primary current distribution.

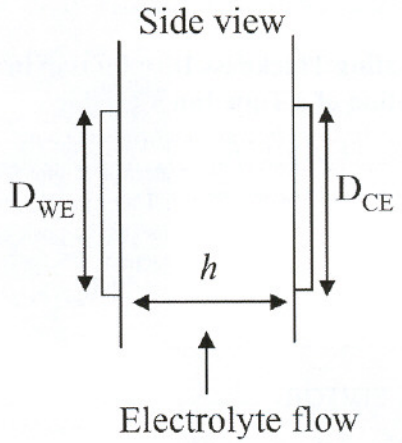

Figure 1—Schematic diagram of the proposed cell side view. The working electrode (WE), as well as the counterelectrode (CE) are assumed to be coplanar with an insulator. The separation distance is assumed to be h.

Experimental

Industrial sodium nitrate ($NaNO_3$) (Chemical Services, Inc., Chicago, IL) was employed to prepare a 200 g/L electrolyte solution used to perform electrochemical machining experiments. Electrolyte conductivity was measured using an Accumet® AP85 portable waterproof conductivity meter.

A custom made cell designed and built in our facilities with a capacity of approximately 125 L of electrolyte solution, was used to perform the electrochemical experiments. The cell included a recirculation flow system with filtration of up to 1 micron particle sizes. The electrolyte flow rate was kept constant at 11.3 L/min (3 gal/min) for all experiments for comparison purposes. Patterned and unpatterned circular areas of 5.0-cm (2-in.) diameter were electrochemically machined using commercially available Hastelloy X and Stainless Steel 303. In the case of unpatterned areas, Hastelloy X was used, whereas for the patterned areas, SS

**Corresponding Author:*
Dr. Alonso Lozano-Morales
Project Engineer
Faraday Technology, Inc.
315 Huls Drive
Clayton, OH 45315
Phone: (937) 836-7749
Fax: (937) 836-9498
E-mail: alonsolozano@faradaytechnology.com

303 was employed. The designed patterned areas consisted of 1.6-mm (1/16-in.) wide strips masked with plating tape and parallel to the electrolyte flow, separated by 3.2-mm (1/8-in.) wide strips exposed for etching. IrO_2-Ta_2O_5-coated titanium material was used as the cathode.

All electrochemical experiments were performed potentiotatically at ambient temperature, using a TecNu rectifier, SPR-300/100/48-3. The applied constant potentials used were 30 and 40 V for patterned and unpatterned areas, respectively. Since, the ratio of counterelectrode to working electrode radii, as well as their separation distance were varied, different current densities were drawn. In order to maintain cell geometry during the experiments, only small amounts of metal were dissolved. Therefore, different electrochemical etching times were employed in order to keep a constant charge of approximately 16 kC, corresponding to a maximum dissolution depth of 0.20 mm (0.008 in).

A Mitutoyo IDS Digimatic Indicator with Absolute Encoder, ID-54012E was used to measure the depth of the circular area etched at five discrete radial positions on pattern and unpatterned areas, perpendicular to the electrolyte flow. Then, the "average" depth was calculated by the sum of the depths at such positions. Finally, the normalized current density was calculated by the ratio of the etch depth at each discrete radial position to the average depth. For some cases, depth profiles were also measured in the direction of fluid flow, and relatively small effects were observed.

Numerical method

It is assumed that the working electrode is in the shape of a disk with radius r_{we}, which is coplanar with an insulator. The counterelectrode is assumed to be of radius r_{ce} and is also coplanar with an insulator. The separation distance is assumed to be h. Figure 1 is a schematic diagram of the proposed cell. Since the purpose of this paper is to comment on cell design, a worst case scenario is treated. Namely, the effect of electrode kinetics,[1] the effect of a slight electrode recess[2] and the impact of plating or etching a patterned feature instead of a continuous feature[4,5] are all neglected. The first two effects would only improve uniformity, and the latter effect would in most cases also improve uniformity. It is therefore unlikely that such phenomena would lead to radical changes in recommendations for cell design.

When h/r_{we} is large, it is well known that current distribution is given by:

$$\frac{i}{i_{avg}} = \frac{0.5}{\sqrt{1-(r/r_{we})^2}} \tag{1}$$

For other cases, the current distribution is calculated numerically using a boundary element method that has been used exensively.[6] Numerical experiments on node point spacing were used to ensure that validity of the results. The semi-infinite domain was modeled as a finite domain by placing an insulating plane at the position $r/r_{we} = 3$. It was confirmed by numerical experiments with different positions of the insulating plane that this approximation introduced neglible changes in the results.

As a means of summarizing results, the following variables were introduced:

$$\Delta = \frac{i(r/r_{we} = 0.9)}{i(r/r_{we} = 0)} \tag{2}$$

and the standard deviation SD in the normalized current density from $r/r_{we} = 0$ to 0.9:

$$SD = \sqrt{\frac{1}{N_w - 1}\sum_{j=1}^{N_w}\left(\frac{i(j) - i_{avg}}{i_{avg}}\right)^2} \tag{3}$$

where N_w is the number of node points on the working electrode between $r/r_{we} = 0$ and 0.9. When the normalized separation distance h/r_{we} is very large, Equation 2 yields $\Delta = 2.29$. Furthermore, $SD = 0.26$ when $N_w = 90$. For this summary, both Δ and SD focused on the middle 90% of the disk because the current density becomes quite high near the edge and, in some applications at least, the regions of the substrate near the edge are either not used or are meant to be sacrificial (essentially acting as current thieves). Conclusions would not change significantly if, for example, the middle 95% of the disk were used in the summary.

Numerical results

Figure 2 shows the calculated current distribution for four ratios of counterelectrode to working electrode radii, assuming $h/r_{we} = 1$. For this separation distance, the counterelectrode radius is important. In all cases, the current distribution is nonuniform, but as the counterelectrode radius shrinks, the current density in the center increases. For significantly larger values of h/r_{we} (for example, values of two or greater), the counterelectrode radius has less influence on the current distribution, and different strategies to improve nonuniformity are required.

For very small values of h/r_{we} (approximately $h/r_{we} < 0.5$), the current density distribution can be rendered relatively uniform for $r_{ce}/r_{we} \sim 1$, as shown in Fig. 3. Deviations from a ratio of one in either direction result in increased nonuniformity.

The normalized current distributions shown in Figs. 2 and 3 show a range of behavior with, in some cases, a minimum in deposition rate just prior to the edge region. Depending on the application, it may not be clear which is the "optimal" current distribution. As a means of summarizing results, the ratio of current densities Δ and the standard deviation SD in the normalized current distribution were used. Figure 4 shows the variation of Δ as a function of the ratio of counterelectrode to working electrode radii for various separation distances. Assuming $\Delta = 1$ is the desired ratio, the results in Fig. 4 would lead to the design recommendations that $r_{ce}/r_{we} \sim 1$ for $h/r_{we} = 0.5$. Furthermore, for all $h/r_{we} < 0.5$, r_{ce}/r_{we} should be approximately one. When $h/r_{we} = 0.75$, a ratio $r_{ce}/r_{we} \sim 0.8$ is optimal, and for $h/r_{we} = 1$, $r_{ce}/r_{we} \sim 0.4$ is "optimal," subject, of course, to other practical constraints such as long-term counterelectrode stability. For separation distances h/r_{we} greater than around one, Δ cannot be reduced to one.

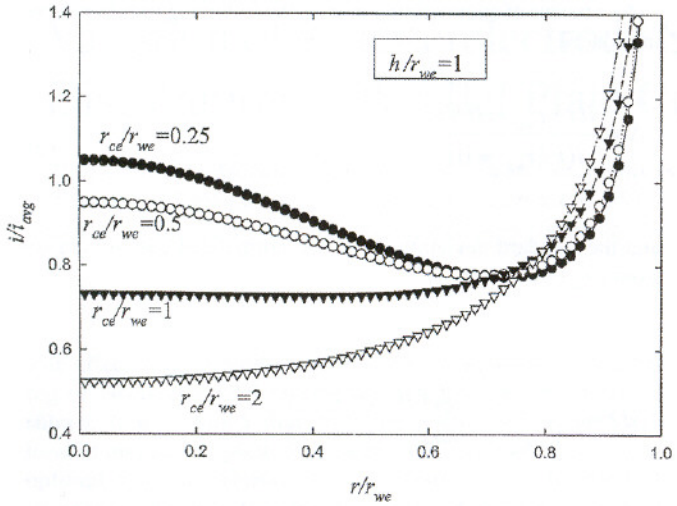

Figure 2—Calculated current distribution for four ratios of counterelectrode to working electrode radii, assuming $h/r_{we} = 1$.

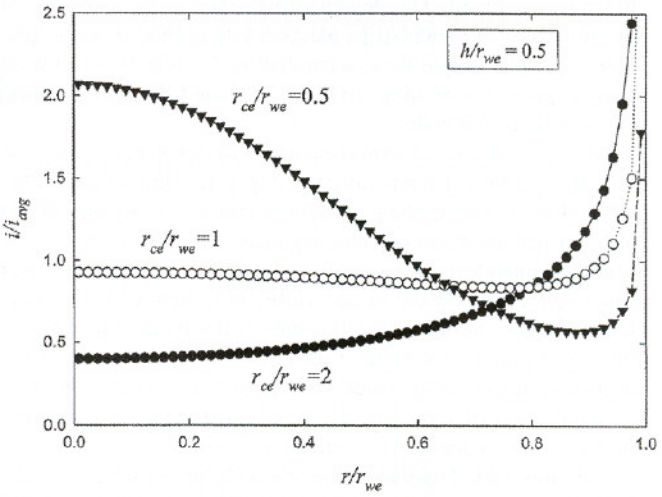

Figure 3—Calculated current distribution for three ratios of counterelectrode to working electrode radii, assuming $h/r_{we} = 0.5$.

If a minimization of *SD* is the better criterion, the recommendations change slightly as seen in Fig. 5. For $h/r_{we} < 1$, the standard deviation experiences a minimum. For $h/r_{we} > 1.25$, it would appear that the smallest practical r_{ce}/r_{we} is desired, and for $h/r_{we} < 0.5$, the recommendation remains that $r_{ce}/r_{we} = 1$.

Comparison with experiment

Simulations were originally performed as an aid to improve uniformity of an electrochemical machining process for Hastelloy X alloy. It is common to drive the machining or electropolishing rates to transport limited rates, helping to ensure a high quality surface finishing.[7-11] Figure 6 shows before and after pictures of the alloy, demonstrating a marked improvement in brightness. A primary current distribution simulation may be relevant to a mass-transfer limited process under certain conditions, and this is therefore a good test case.

Figure 7 indeed shows a comparison of simulation with experiment for three test geometries, two of which were chosen to yield a relatively uniform distribution in machining rate. In Fig. 7, the "average" current density was calculated in the exact manner of the experiments to allow for a comparison. The "average" was simply calculated by a sum of the current densities at five discrete radial positions. For this reason, the normalized current density differs from those shown in Figs. 2 and 3, where the area-average current density is shown, which provides greater weight to current densities at larger radii.

Results are shown for three cell geometries. The cell geometries in Figs. 7a and 7c were set to yield a relatively uniform current distribution relative to the geometry in Fig. 7b. In all cases, the experimental and simulated results are in good agreement, especially considering that the mass-transfer limitations may have been expected to play a role. Experimentally, measurements were taken at radial positions perpendicular to the direction of flow as a means of minimizing any effects associated with spatial variations in boundary-layer thickness resulting from the fluid flow. When measurements were taken in the direction of flow, results were largely unchanged.

Figure 8 shows a comparison of simulation with experimental for three test geometries on circular patterned areas (note, also SS 303 was used instead of Hastelloy X). The "average" current density was calculated in the same manner as for results shown in Fig. 7. Results are shown for three cell geometries. The cell geometry in Fig. 8c ($h/r_{we} = 1$, $r_{ce}/r_{we} = 1$) was set to yield a relatively uniform current distribution relative to the cell geometry in Figs. 8a ($h/r_{we} = 2$, $r_{ce}/r_{we} = 1$) and 8b ($h/r_{we} = 0.75$, $r_{ce}/r_{we} = 0.25$). In contrast to the results in Fig. 7, the experimental and simulated results are in only fair agreement, but clearly trends are captured by the simulations, even if the patterning is not taken into consideration. While not exhaustive, the present example helps to demonstrate that the simple design calculations summarized in Figs. 4 and 5 can be used to set the counterelectrode size even when the circular regions are patterned.

Conclusions

Depending on the separation distance between anode and cathode, the ratio of electrode sizes can be used to minimize nonuniformities in the current distribution on the working electrode. When $h/r_{we} > 1.25$, it would appear that the smallest practical r_{ce}/r_{we} is desired, and for $h/r_{we} < 0.5$, $r_{ce}/r_{we} = 1$ should be optimal. For intermediate values of h/r_{we}, the best ratio can be estimated from either Figs. 4 or 5.

Acknowledgement

This work was supported in part under the National Science Foundation's Small Business Technology Transfer program, Award No. IIP-0711332.

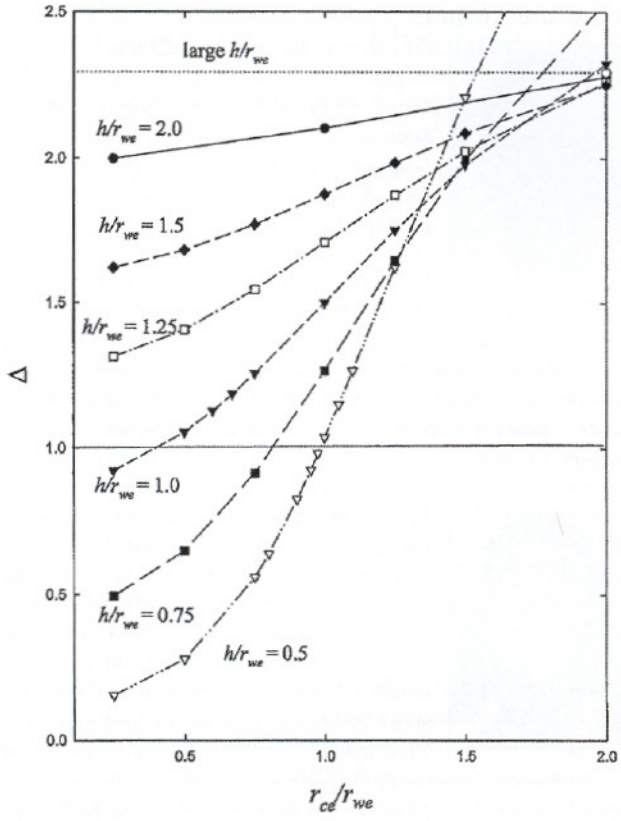

Figure 4—Variation of Δ as a function of the ratio of counterelectrode to working electrode radii for various separation distances.

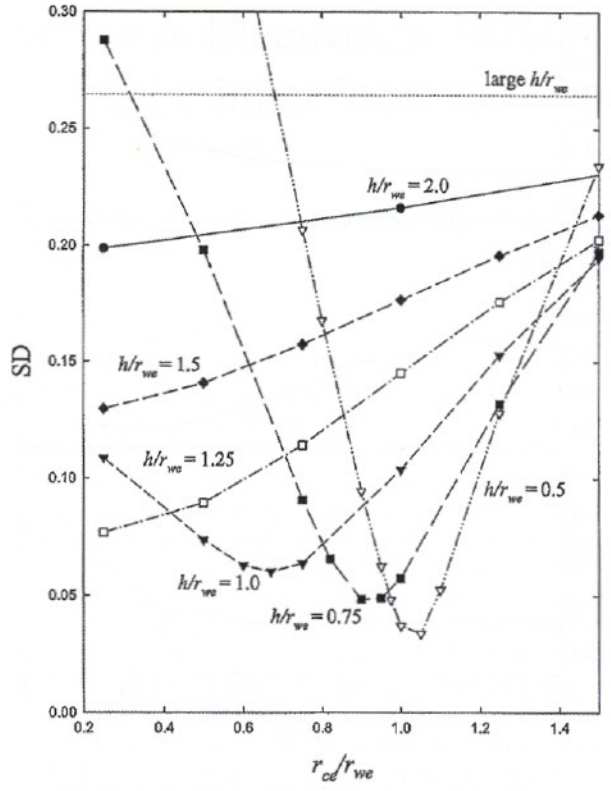

Figure 5—Variation of standard deviation (SD) as a function of the ratio of counterelectrode to working electrode radii for various separation distances.

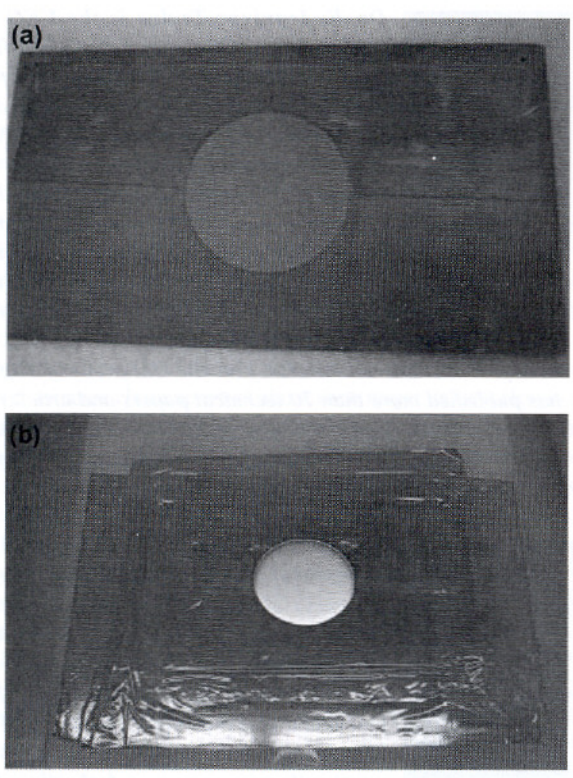

Figure 6—Pictures of the before (a) and after (b) electrochemical machining surface finish of Hastelloy X, with a circular unpatterned area of 2 in.

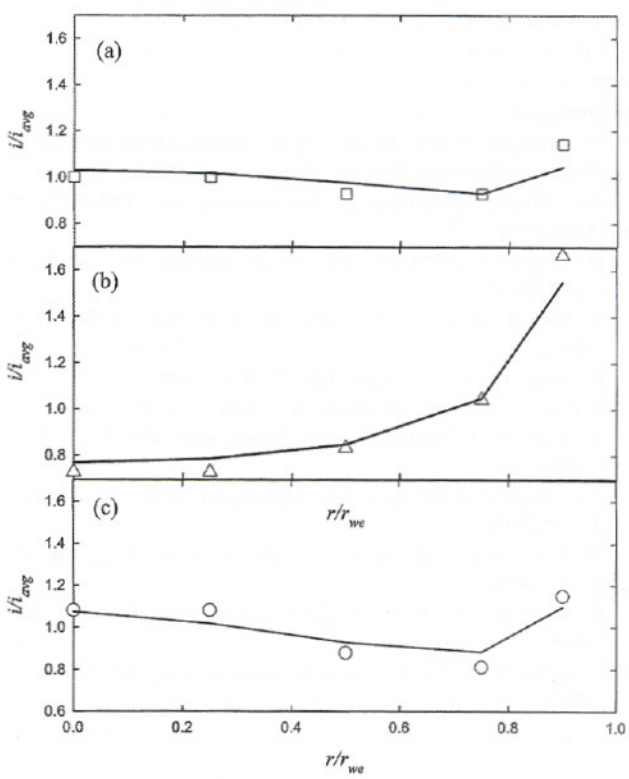

Figure 7—Comparison of the simulated normalized current density with experiment for three test geometries: (a) h/r_{we} = 0.5, r_{ce}/r_{we} = 1, (b) h/r_{we} = 2, r_{ce}/r_{we} = 1, (c) h/r_{we} = 1, r_{ce}/r_{we} = 0.5, using Hastelloy X with unpatterned circular areas.

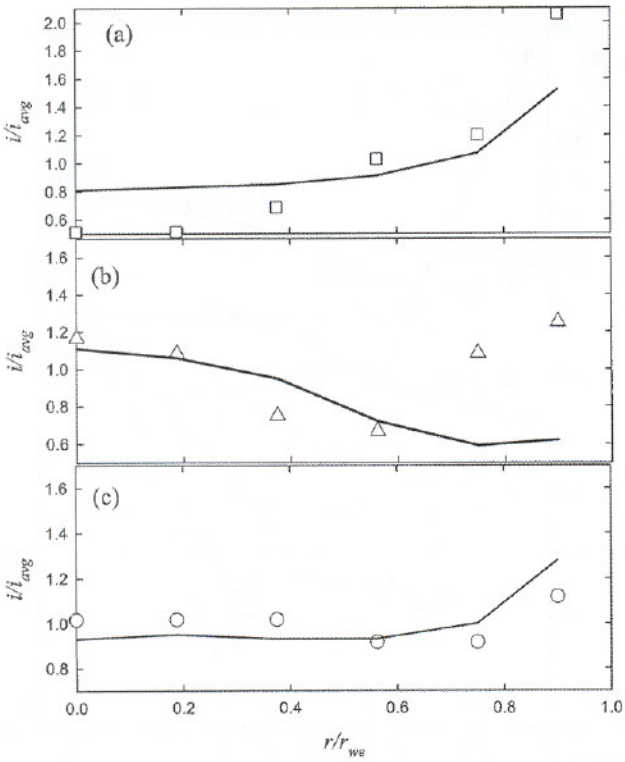

Figure 8—Comparison of the simulated normalized current density with experiment for three test geometries: (a) $h/r_{we} = 2$, $r_{ce}/r_{we} = 1$, (b) $h/r_{we} = 0.75$, $r_{ce}/r_{we} = 0.25$, (c) $h/r_{we} = 1$, $r_{ce}/r_{we} = 1$, using SS 303 with patterned circular areas.

References

1. J.S. Newman & K.E. Thomas-Alyea, *Electrochemical Systems, 3rd Ed.*, John Wiley & Sons, Hoboken, NJ, 2004.
2. A.C. West & J. Newman, *J. Electrochem. Soc.*, **138** (6), 1620 (1991).
3. H. Lavelaine de Maubeuge, *J. Electrochem. Soc.*, **149** (8), C413 (2002).
4. S. Mehdizadeh, *et al.*, *J. Electrochem. Soc.*, **139** (1), 78 (1992).
5. B. DeBecker & A.C. West, **143** (2), 486 (1996).
6. Y. Cao, *et al.*, *J. Electrochem. Soc.*, **148** (7), C466 (2001).
7. M. Datta & D. Landolt, *Electrochimica Acta*, **45** (15-16), 2535 (2000).
8. A.C. West, P. Andricacos & L. Deligianni, *IBM J. Res. Devel.*, **49**, 37 (2005).
9. M. Datta & L.T. Romankiw, *J. Electrochem. Soc.*, **136** (6), 285C (1989).
10. R. Vidal & A.C. West, *J. Electrochem. Soc.*, **142** (8), 2689 (1995).
11. C. Clerc & D. Landolt, *Electrochimica Acta*, **32** (10), 1435 (1987).

About the Authors

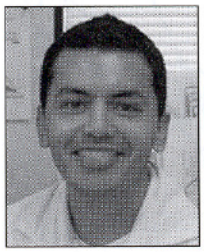

Dr. Alonso Lozano-Morales is a Project Engineer at Faraday Technology, Inc. He received his B.S. from Universidad de Sonora, Mexico and his Ph.D. degree from Louisiana State University, Baton Rouge, LA. All the above degrees are from the Department of Chemical Engineering. Dr. Lozano-Morales' Ph.D. thesis titled, Electrodeposition of Nanocomposites as Thin Films and HARMs for MEMS, *involved the electrochemical deposition of nanocomposite metal alloys, catalyzation of metal foams and modeling of electrochemical deposition processes. Currently, he is leading Faraday Technology's edge and surface finishing process technology development, as well as industrial coatings.*

Ms. Heather A. McCrabb is a Project Engineer at Faraday Technology, Inc., Clayton, OH. She received her B.S. and M.S. degrees in Chemistry at Wright State University, Dayton, OH, in 1999 and 2001, respectively. Currently, Ms. McCrabb is leading Faraday's efforts in the development of electrodeposition processes for VLSI applications and the development of electrophoretic deposition processes for coating applications. Her Master's thesis involved work with the synthesis, characterization, and electrochemical studies of multiple room temperature ionic liquids for application as electrolytes in lithium ion batteries. Ms. McCrabb is a member of the American Chemical Society.

Dr. E. Jennings Taylor is the CEO and IP Director at Faraday Technology, Inc., Clayton, OH. He founded the company to develop and commercialize innovative electrochemical technology using sophisticated charge-modulated electric fields. The company's intellectual property has been successfully transferred both to government agencies and large manufacturers in the form of process engineering technology and products. He holds a B.A. in chemistry from Wittenberg University, an M.A. in technology strategy and policy from Boston University, and M.S. and Ph.D. degrees in materials science from the University of Virginia. He has published more than 70 technical papers and articles and holds many patents. He currently serves as Chairman of the AESF Foundation Research Board. He is the 2007 recipient of the William Blum AESF Scientific Achievement Award.

Dr. Alan C. West is a Professor in the Department of Chemical Engineering, Columbia University, New York. He earned his B.S. in Chemical Engineering from Case Western Reserve University in 1985 and his Ph.D in Chemical Engineering from University of California, Berkeley in 1989. His research interests include electrochemical metallization processes, fuel cells, batteries and microfluidics.